analytical chemistry

ARTICLE

pubs.acs.org/ac

Spin-Trapping Reactions of a Novel Gauchetype Radical Trapper G-CYPMPO

Toshitaka Oka,[*,†] Shinichi Yamashita,[‡] Masamichi Midorikawa,[¶] Seiichi Saiki,[‡] Yusa Muroya,[§] Masato Kamibayashi,[∥] Masayuki Yamashita,[∥] Kazunori Anzai,[⊥] and Yosuke Katsumura[*,¶]

[†]Advanced Science Research Center, Japan Atomic Energy Agency (JAEA), Tokai-mura, Ibaraki 319−1195, Japan

[‡]Quantum Beam Science Directorate, Japan Atomic Energy Agency (JAEA), Takasaki, Gunma 370−1292, Japan

[¶]School of Engineering, The University of Tokyo, Bunkyo, Tokyo 113−8656, Japan

[§]School of Engineering, The University of Tokyo, Tokai-mura, Ibaraki 319−1188, Japan

[∥]Pharmaceutical Manufacturing Chemistry, Kyoto Pharmaceutical University, Kyoto, Kyoto 607−8414, Japan

[⊥]School of Pharmaceutical Sciences, Nihon Pharmaceutical University, Kitaadachi, Saitama 362−0806, Japan

ABSTRACT: Chemical reactions of a novel gauchetype spin trap, G-CYPMPO (*sc*-5-(5,5-dimethyl-2-oxo-1,3,2-dioxaphosphinan-2-yl)-5-methy-1-pyrroline *N*-oxide, O1−P1−C6−N1 torsion angle = 52.8°), with reactive oxygen species were examined by pulse radiolysis technique with 35 MeV electron beam and by electron spin resonance spectroscopy after ^{60}Co γ-ray irradiation. The spin-trapping reaction rate constants of G-CYPMPO toward the hydroxyl radical and the hydrated electron were estimated to be $(4.2 \pm 0.1) \times 10^9$ and $(11.8 \pm 0.2) \times 10^9$ $M^{-1}s^{-1}$, respectively. Half-lives of the spin adducts, hydroxyl radical, and perhydroxyl radical adducted G-CYPMPO were estimated to be ∼35 and ∼90 min, respectively. A comparison of the results with earlier reports using different radical sources suggests that the purity of the solution and/or the radical generation technique may influence the stability of the spin adducts.

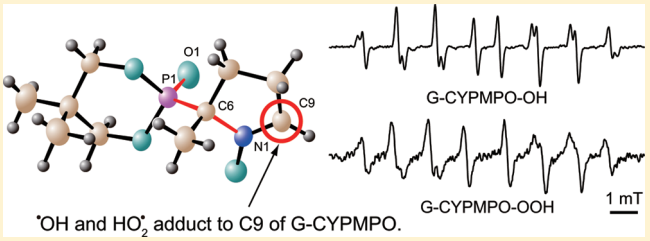

Reactive oxygen species (ROS), such as the hydroxyl radical ($^{\bullet}$OH), the superoxide anion radical ($O_2^{\bullet-}$), and the perhydroxyl radical ($HO_2^{\bullet}$), are well-known to play a crucial role in biological damages such as DNA strand breaks, heart attack, cancer, ischemia-reperfusion injury, and so on.[1−4] The detection and quantification of these oxygen-derived free radicals in biological systems is very important for an accurate evaluation and understanding of these diseases.[5−7]

These radicals can be produced not only by an enzymatic reaction in a biological system, but also in water radiolysis. The estimation of these radical productions in water radiolysis is also important, because it can offer useful information for ion-beam radiation therapy. Baldacchino et al. determined the yield of $^{\bullet}$OH using a fluorescent probe,[8] and LaVerne et al. estimated the yield of $HO_2^{\bullet}$ from water radiolysis by heavy ion-beams.[9] Meesungnoen et al. calculated the yields and concentrations of O_2 in ion-beam tracks by Monte Carlo simulation.[10]

One of the most sensitive and definitive methods to detect these free radicals is a spin-trapping method utilizing electron spin resonance (ESR) spectroscopy.[11] With this technique, very short-lived oxygen derived radicals ($^{\bullet}$OH, $O_2^{\bullet-}$, $HO_2^{\bullet}$, etc.) react with a spin trap and form rather long-lived radicals. DMPO (5,5-dimethyl-1-pyrroline *N*-oxide) has been most widely used as a spin trap to identify and quantify the oxygen-derived free radicals,[12,13] but it has several drawbacks, such as handling difficulties due to its low melting point (35 °C), ready development of free-radical impurities under ambient conditions, and short lifetime of $O_2^{\bullet-}$ adduct.[14]

To overcome these drawbacks, a cyclic DEPMPO (5-diethoxyphosphoryl-5-methyl-1-pyrroline *N*-oxide)-type novel spin trap, CYPMPO (CAS No. 934182-09-9) was obtained as a slightly hydroscopic colorless crystalline compound (mp 126 °C) that was determined to be an antitype conformation[14] and was evaluated for spin-trapping capabilities.[14,15] The conformation of CYPMPO was determined to be an antitype, in which the O1−P1−C6−N1 torsion angle of CYPMPO was 164.31°. Recently, one of the authors, Kamibayashi, successfully synthesized a nonhygroscopic new spin trap, G-CYPMPO (*sc*-5-(5,5-dimethyl-2-oxo-1,3,2-dioxaphosphinan-2-yl)-5-methy-1-pyrroline *N*-oxide) which has a gauche conformation as shown in Figure 1a. Kitamura et al. reported that G-CYPMPO attenuates the neuro-degeneration in a rat Parkinson's disease model.[16] Moreover, G-CYPMPO aqueous solution can be stored under ambient conditions for at least one month without any development of free-radical impurities. These results suggest that G-CYPMPO is a useful tool in biochemical research, better than either DMPO or DEPMPO, and widespread research using G-CYPMPO is expected. However, details of the chemical reaction

Received: September 9, 2011
Accepted: October 19, 2011
Published: October 19, 2011

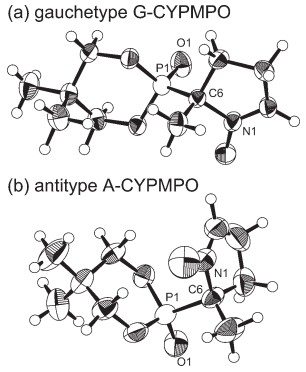

Figure 1. X-ray structure analysis of (a) a novel gauchetype spin-trap G-CYPMPO and (b) antitype A-CYPMPO. The torsion angle was determined from the O1−P1−C6−N1 angle.

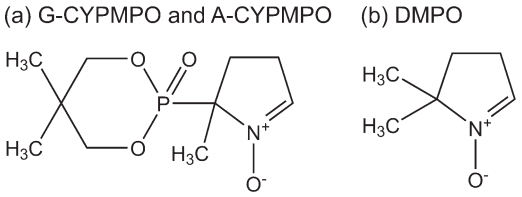

Figure 2. Chemical structures of (a) G-CYPMPO and A-CYPMPO and (b) DMPO.

between G-CYPMPO and the oxygen-derived free radicals are less understood. In the present paper, we report rate constants of G-CYPMPO toward reactive species and lifetime of spin-adducted G-CYPMPO. The reactive species such as hydrated electrons (e_{aq}^-), $^{\bullet}OH$ and $HO_2^{\bullet}$ were generated by water radiolysis. The rate constants were studied by pulse radiolysis method, whereas identification and lifetime estimation of G-CYPMPO adducts were followed by ESR spectroscopy.

MATERIALS AND METHODS

Chemicals. A colorless needle-shaped spin trap, G-CYPMPO, anti-CYPMPO (A-CYPMPO, *ap*-5-(5,5-dimethyl-2-oxo-1,3,2-dioxaphosphinan-2-yl)-5-methy-1-pyrroline *N*-oxide), and one of the most popular spin traps (DMPO, the chemical structures of which are shown in Figure 2) were used. G-CYPMPO was synthesized by oxidizing CYPMPH (*ap*-2-(5,5-dimethyl-2-oxo-1,3,2-dioxaphosphinan-2-yl)-2-methylpyrrolidine, CAS No. 902503-51-9) in diluted hydrogen peroxide in the presence of a catalytic amount of sodium tungstate and purified by silica gel column chromatography.[16] X-ray structure analysis of G-CYPMPO (mp 127.8−128.6 °C) and highly purified A-CYPMPO (mp 130 °C) were performed utilizing a R-AXIS RAPID II X-ray diffractometer (Rigaku, Japan).

All aqueous solutions were prepared with ultrapure water from a Milli-Q system (Millipore, Bedford, MA), and saturated with highly pure N_2O, Ar, or O_2 gases by bubbling for ~30 min before irradiation. N_2O and Ar gases were used to enable the conversion of e_{aq}^- to $^{\bullet}OH$, via the reaction[17,18]

$$e_{aq}^- + N_2O + H_2O \rightarrow N_2 + {}^{\bullet}OH + OH^-$$

or to remove dissolved O_2, respectively. *Tert*-butyl alcohol (*t*-BuOH) and formic acid (HCOOH) were added as a scavenger for $^{\bullet}OH$[19] in pulse radiolysis experiment and ESR measurement, respectively.

Table 1. O1−P1−C6−N1 Torsion Angle and Wavenumber of Specific IR Peak for A-CYPMPO and G-CYPMPO

spin trap	torsion angle/°	IR (KBr)/cm^{-1}
G-CYPMPO	52.8	1579.6
A-CYPMPO	164.57	1573.8

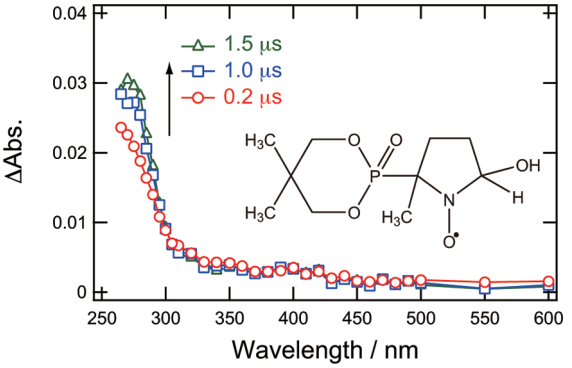

Figure 3. Transient absorption spectra of G-CYPMPO−OH. ΔAbs. increases with increasing time from irradiation. Inset shows the chemical structure of G-CYPMPO−OH.

Electron Pulse Radiolysis. Pulse radiolysis experiments were conducted at LINAC, the electron linear accelerator at the Nuclear Professional School, University of Tokyo. The energy and pulse duration of the electron beam were 35 MeV and 10 ns, respectively. The average dose per pulse was 10−45 Gy, which was measured with an N_2O-saturated 10 mM KSCN aqueous solution.[18−20] The apparatus has been described in a previous article.[21] G-CYPMPO aqueous solution in a quartz cell with a 20-mm optical path was irradiated at room temperature (ca. 20 °C).

***γ*-ray Irradiation and an ESR Measurement.** G-CYPMPO aqueous solutions were irradiated with *γ*-rays from the ^{60}Co *γ*-ray source at the University of Tokyo. Dosimetry was done preliminarily with the Fricke dosimeter; the dose rate was ca. 7 Gy/min, and the dose was set to 200 Gy. After irradiation, the solutions were immediately transferred from a glass tube irradiation cell to a quartz ESR flat cell and placed into the ESR cavity. ESR measurements were performed utilizing a Model JES-RE2X ESR spectrometer (JEOL, Tokyo, Japan) with a microwave power of 1 mW, a modulation width of 0.1 mT, a time constant of 0.1 s, a sweep time of 2−15 min, and the peak-to-peak intensities of the spin adducts were observed. All the irradiation and measurement were carried out at room temperature (ca. 25 °C).

RESULTS AND DISCUSSION

X-ray Structure Analysis. Figure 1 shows the results of the X-ray structure analysis for G-CYPMPO and A-CYPMPO, and the O1−P1−C6−N1 torsion angles are listed in Table 1. A torsion angle of 52.8° for G-CYPMPO indicates that the conformation of G-CYPMPO is gauche, whereas the torsion angle of A-CYPMPO is 164.57°.

Rate Constant Determination. Since e_{aq}^- is scavenged by dissolved N_2O and converted to $^{\bullet}OH$ in N_2O-saturated aqueous solution, only the behavior of $^{\bullet}OH$ can be observed. Figure 3

dx.doi.org/10.1021/ac2023926 |*Anal. Chem.* 2011, 83, 9600–9604

Table 2. Rate Constants (10^9 $M^{-1}s^{-1}$) for G-CYPMPO, A-CYPMPO, and DMPO toward $^{\bullet}OH$ Observed by a Competition Method and e^-_{aq} Measured at 715 nm

spin trap		$^{\bullet}OH/10^9$ $M^{-1}s^{-1}$	$e^-_{aq}/10^9$ $M^{-1}s^{-1}$
G-CYPMPO	this work	4.2 ± 0.1	11.8 ± 0.2
A-CYPMPO	reported[15]	>1	
DMPO	this work	4.0 ± 0.1	8.3 ± 0.1
	reported[17]	4.0	

shows transient absorption spectra observed in pulse radiolysis of an N_2O-saturated 0.3-mM G-CYPMPO aqueous solution at different elapsed times from the electron beam irradiation. Each spectrum shows a strong absorption below 300 nm and a weak broad peak at ~400 nm, whereas unirradiated CYPMPO has an absorption peak at λ = 233 nm but not at λ > 270 nm. These peaks can be attributed to an $^{\bullet}OH$ adduct of G-CYPMPO, G-CYPMPO−OH, the chemical structure of which is shown in the inset of Figure 3. $^{\bullet}OH$ itself also has an absorption band below 300 nm and it survives ~2 μs after electron beam irradiation in pure water,[22,23] so that both the production of G-CYPMPO−OH and the consumption of $^{\bullet}OH$ appear in the time region of Figure 3. However, it is confirmed by a competition method with a thiocyanate anion as described hereinafter that G-CYPMPO reacts with $^{\bullet}OH$ at a diffusion-controlled rate constant, leading to identification of the observed peak as absorption of G-CYPMPO−OH. Similar transient spectra were obtained for DMPO−OH, suggesting that the reaction sites of these spin traps for $^{\bullet}OH$ scavenging are same. By spin trapping, $^{\bullet}OH$ adducts to the carbon of the C=N bond in a pyrroline-ring (Figure 2), and the spin trap itself becomes a radical.

On the other hand, reaction with e^-_{aq} was observed by removing $^{\bullet}OH$ via the addition of 100 mM *t*-BuOH. Sample solutions were saturated with argon to purge O_2, because O_2 scavenges e^-_{aq} rapidly with a reaction rate constant of 1.9×10^{10} $M^{-1}s^{-1}$.[17] The transient absorption spectra of e^-_{aq} were observed, and the well-known absorption peak of e^-_{aq} was confirmed at ~715 nm.[23,24] This peak decays with first-order kinetics in the presence of G-CYPMPO, while the decay without G-CYPMPO is known to be second-order kinetics. The first-order reaction rate increases as the G-CYPMPO concentration increases, showing that e^-_{aq} is scavenged by G-CYPMPO. Generally, the decay time of e^-_{aq} in pure water is longer than 1.5 μs,[25,26] such e^-_{aq} decrement is due to the reaction of that with G-CYPMPO. No other species were observed by this reaction in the UV−vis domain (λ = 265−800 nm). A similar tendency was observed from the transient spectra for e^-_{aq} in the DMPO.

Because of the overlap of the production of G-CYPMPO−OH and the consumption of $^{\bullet}OH$ (Figure 3), the rate constant of G-CYPMPO toward $^{\bullet}OH$ was obtained via a competition method, using KSCN as a reference, not by build-up kinetics analysis. The reference reaction rate constant for SCN^- + OH was 1.1×10^{10} $M^{-1}s^{-1}$.[17] By varying the ratio of the concentration of G-CYPMPO to that of KSCN, the rate constant was estimated to be $(4.2 \pm 0.1) \times 10^9$ $M^{-1}s^{-1}$. The reported rate constant of A-CYPMPO, estimated using a competitive-trapping method with ESR, was larger than 10^9 $M^{-1}s^{-1}$.[15] Our result is consistent with the previous data, but more precise. On the other hand, the rate constant of G-CYPMPO toward e^-_{aq} was $(11.8 \pm 0.2) \times 10^9$ M^{-1} s^{-1}, determined from the time profiles recorded at 715 nm with different G-CYPMPO concentrations.

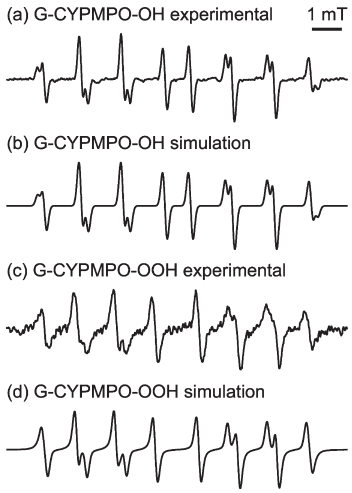

Figure 4. ESR spectra of G-CYPMPO−OH and G-CYPMPO−OOH. For G-CYPMPO−OH: (a) experimental spectrum generated with γ-ray irradiation of a G-CYPMPO aqueous solution bubbled with N_2O, and (b) corresponding computer-simulated spectrum considering two diastereomers. For G-CYPMPO−OOH: (c) experimental spectrum generated by γ-ray irradiation of a G-CYPMPO aqueous solution with HCOOH bubbled with O_2 gas, and (d) corresponding computer-simulated spectrum considering two diastereomers.

Table 3. Hyperfine Coupling Constants (hfcc) of G-CYPMPO−OH and G-CYPMPO−OOH Used for the Simulation Spectra in Figure 4

spin adduct	diastereomer	A_N/mT	A_H/mT	A_P/mT
G-CYPMPO−OH	A	1.40	1.40	5.04
	B	1.40	1.22	4.90
G-CYPMPO−OOH	A	1.32	1.04	5.11
	B	1.30	1.15	5.24

The rate constants obtained in this work are listed in Table 2, along with those for DMPO. The rate constants of G-CYPMPO/DMPO toward $^{\bullet}OH$ are comparable, whereas the rate constant for G-CYPMPO with e^-_{aq} is notably higher than that for DMPO with regard to e^-_{aq}, suggesting that reaction sites of e^-_{aq} scavenging might be different for DMPO and G-CYPMPO.

Selective Detection of Spin Adducts. An ESR spectrum for G-CYPMPO−OH of a 1.0 mM G-CYPMPO aqueous solution saturated with N_2O gas irradiated with γ-rays and the corresponding computer simulated spectrum are shown in Figures 4a and 4b, respectively. The simulated spectrum was drawn using two sets of hyperfine coupling constants (hfcc), representing two diastereomers[15] of G-CYPMPO−OH, summarized in Table 3. The experimental spectrum consists of two identical groups of lines which are split by a large hyperfine coupling with phosphorus, and is similar to the ESR spectra of the $^{\bullet}OH$ and $HO_2^{\bullet}$ adducts trapped by DEPMPO and A-CYPMPO. On the other hand, Figures 4c and 4d represent an experimental ESR spectrum for G-CYPMPO-OOH and the corresponding computer simulated spectrum, respectively. A 1.0 mM G-CYPMPO/200 mM HCOOH aqueous solution under acidic conditions was bubbled with O_2 gas and then irradiated with γ-ray. The hfccs used in the simulation of Figure 4d are also listed in Table 3. Compared to

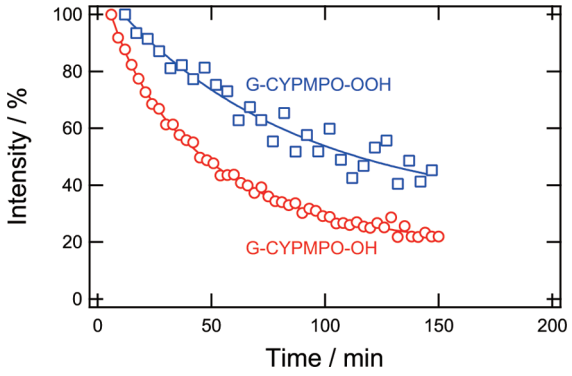

Figure 5. Decay of the ESR signal for G-CYPMPO−OH and G-CYPMPO−OOH after γ-ray irradiation. The peak-to-peak intensity of the fourth peak from the left in the ESR spectra was plotted versus time elapsed after irradiation. The decay curves are fitted by double exponential.

the hfcc of CYPMPO−OH and CYPMPO−OOH,[15] the relatively wide hfccs of phosphorus A_P (2.0%−4.3% wider) may be due to the difference of the conformation observed for G-CYPMPO−OH and G-CYPMPO−OOH.

Figure 5 displays the variations of the peak-to-peak intensities of the G-CYPMPO−OH and G-CYPMPO−OOH as a function of elapsed time from γ-ray irradiation. All the data are normalized at the first-derivative intensities of each spin adduct. The decay rate of G-CYPMPO−OH is faster than that of G-CYPMPO-OOH. The decay curves are fitted by double exponential and the half-lives of the G-CYPMPO−OH and G-CYPMPO−OOH are estimated to be ∼35 and ∼90 min, respectively, using the faster components. Previously, Saito et al. reported that the half-lives of CYPMPO−OH and CYPMPO−OOH were 44.8 and 30.4 min, respectively.[27] In that report, $^{\bullet}$OH was generated by irradiation with 1.0 MHz ultrasound without any additives. In our case, $^{\bullet}$OH was generated by γ-ray irradiation without any additives. Both techniques may produce "pure" $^{\bullet}$OH, so that the difference between the previous result and present result is smaller than that of G-CYPMPO−OOH. The half-life of G-CYPMPO−OOH in the present work is quite different from that of the previous report. In the previous work, $HO_2^{\bullet}$ was generated from the hypoxanthine/xanthine oxidase (HPX/XOD) aqueous system with dimethyl sulfoxide (DMSO) and phosphate buffer added. In contrast to such an enzymatic reaction, in γ-ray irradiation method, only one $^{\bullet}$OH scavenger is used. Maybe because of the difference between the additive and radical generation method, the half-life of G-CYPMPO−OOH of the present work is obviously longer than that of the previous work.[27] Moreover, the yield of G-CYPMPO−OOH is quite low, compared to that of G-CYPMPO−OH. One can see the relatively large dispersion of G-CYPMPO−OOH data in Figure 5, which is due to the low concentration of the adduct. A higher concentration of the G-CYPMPO−OOH is required for an accurate evaluation of the function of oxygen-derived radicals in a living body. The relationship between the decay behavior and the dose effect/dose rate effect for spin trapping of G-CYPMPO is also important. Further study will be required on these points.

CONCLUSION

The X-ray structure analysis of G-CYPMPO and determination of the rate constants of G-CYPMPO toward $^{\bullet}$OH and e_{aq}^- were carried out by X-ray diffraction, pulse radiolysis technique, and the trapping of oxygen-derived radicals with G-CYPMPO, and their decay was investigated by ESR spectroscopy, which are useful for the accurate evaluation of the function of ROS in the living body. From the X-ray structure analysis, we determined the O1−P1−C6−N1 torsion angle of 52.8°. The trapping reactions are all diffusion-controlled and we found that the rate constant for G-CYPMPO with e_{aq}^- is larger than that for DMPO. The hyperfine coupling constants for G-CYPMPO−OH and G-CYPMPO-OOH are relatively higher than those for CYPMPO−OH and CYPMPO−OOH. Half-lives of G-CYPMPO−OH and G-CYPMPO−OOH are estimated to be 35 and 90 min, respectively. The half-life of G-CYPMPO−OOH generated by a "pure" method becomes longer than the half-life of CYPMPO−OOH generated by an enzymatic reaction, indicating that the additive plays an important role in the stability of the G-CYPMPO adduct.

AUTHOR INFORMATION

Corresponding Author

*E-mail addresses: oka.toshitaka@jaea.go.jp (T.O.), katsu@n.t.u-tokyo.ac.jp (Y.K.).

ACKNOWLEDGMENT

Authors thank Mr. D. Hiroishi, Mr. T. Ueda, and Prof. M. Uesaka (University of Tokyo) for their technical assistance in γ-ray irradiation and pulse radiolysis experiments.

REFERENCES

(1) Roubaud, V.; Sankarapandi, S.; Kuppusamy, P.; Tordo, P.; Zweier, J. L. *Anal. Biochem.* **1997**, *247*, 404–411.
(2) Fridovich, I. *Annu. Rev. Pharmacol. Toxicol.* **1983**, *23*, 239–257.
(3) Valko, M.; Leibfritz, D.; Moncol, J.; Cronin, M. T. D.; Mazur, M.; Telser, J. *Int. J. Biochem. Cell Biol.* **2007**, *39*, 44–84.
(4) Valacchi, G., Davis, P. A., Eds. *Oxidants in Biology: A Question of Balance*, 1st ed.; Springer: Berlin, Heidelberg, 2008.
(5) Maurelli, E.; Culcasi, M.; Delmas-Beauvieux, M. C.; Miollan, M.; Gallis, J. L.; Tron, T.; Pietri, S. *Free Radic. Biol. Med.* **1999**, *27*, 34–41.
(6) Samouilov, A.; Roubaud, V.; Kuppusamya, P.; Zweier, J. L. *Anal. Biochem.* **2004**, *334*, 145–154.
(7) Hardy, M.; Rockenbauer, A.; Vasquez-Vivar, J.; Felix, C.; Lopez, M.; Srinivasan, S.; Avadhani, N.; Tordo, P.; Kalyanaraman, B. *Chem. Res. Toxicol.* **2007**, *20*, 1053–1060.
(8) Baldacchino, G.; Maeyama, T.; Yamashita, S.; Taguchi, M.; Kimura, A.; Katsumura, Y.; Murakami, T. *Chem. Phys. Lett.* **2009**, *468*, 275–279.
(9) LaVerne, J. A.; Schuler, R. H.; Burns, W. G. *J. Phys. Chem.* **1986**, *90*, 3238–3242.
(10) Meesungnoen, J.; Jay-Gerin, J. P. *Radiat. Res.* **2009**, *171*, 379–386.
(11) Janzen, E. G.; Blackburn, B. J. *J. Am. Chem. Soc.* **1969**, *91*, 4481–4490.
(12) Timmins, G. S.; Liu, K. J.; Bechara, E. J. H.; Kotake, Y.; Swartz, H. M. *Free Radicals Biol. Med.* **1999**, *27*, 329–333.
(13) Anzai, K.; Aikawa, T.; Furukawa, Y.; Matsushima, Y.; Urano, S.; Ozawa, T. *Arch. Biochem. Biophys.* **2003**, *415*, 251–256.
(14) Nakanishi, Y.; Ikota, N.; Yakumaru, H.; Chichii, M.; C, N.; Ozawa, T.; Kameda, H.; Okada, T.; Ohta, S.; Yamasita, M.; Kawasaki, I.; Kamibayashi, M. *Proceedings of the 126th Annual meetings of the Pharmaceutical Society of Japan*, 2006, Paper No. P28[Q]pm-74.
(15) Kamibayashi, M.; Oowada, S.; Kameda, H.; Okada, T.; Inanami, O.; Ohta, S.; Ozawa, T.; Makino, K.; Kotake, Y. *Free Radical Res.* **2006**, *40*, 1166–1172.

(16) Kitamura, Y.; Kamibayashi, M.; Inden, M.; Yanagida, T.; Shibaike, T.; Takata, K.; Yasui, H.; Yamashita, M.; Taniguchi, T. *Neurochem. Int.* **2011**, *58*, 721–727.
(17) Buxton, G. V.; Greenstock, C. L.; Helman, W. P.; Ross, A. B. *J. Phys. Chem. Ref. Data* **1988**, *17*, 513–886.
(18) Hata, K.; Lin, M. Z.; Katsumura, Y.; Muroya, Y.; Fu, H. Y.; Yamashita, S.; Nakagawa, H. *J. Radiat. Res.* **2011**, *52*, 15–23.
(19) Mostafavi, M.; Lin, M. Z.; Wu, G. Z.; Katsumura, Y.; Muroya, Y. *J. Phys. Chem. A* **2002**, *106*, 3123–3127.
(20) Buxton, G. V.; Stuart, C. R. *J. Chem. Soc.—Faraday Trans.* **1995**, *91*, 279–281.
(21) Muroya, Y.; Lin, M. Z.; de Waele, V.; Hatano, Y.; Katsumura, Y.; Mostafavi, M. *J. Phys. Chem. Lett.* **2010**, *1*, 331–335.
(22) Nielsen, S. O.; Michael, B. D.; Hart, E. J. *J. Phys. Chem.* **1976**, *80*, 2482–2488.
(23) Boyle, J. W.; Ghormley, J. A.; Hochanadel, C. J.; Riley, J. F. *J. Phys. Chem.* **1969**, *73*, 2886–2890.
(24) Jou, F.-Y.; Freeman, G. R. *J. Phys. Chem.* **1977**, *81*, 909–915.
(25) Trumbore, C. N.; Youngblade, W.; Short, D. R. *J. Phys. Chem.* **1984**, *88*, 5057–5061.
(26) Wu, G. Z.; Katsumura, Y.; Muroya, Y.; Li, X. F.; Terada, Y. *Radiat. Phys. Chem.* **2001**, *60*, 395–398.
(27) Saito, K.; Takahashi, M.; Kamibayashi, M.; Ozawa, T.; Kohno, M. *Free Radical Res.* **2009**, *43*, 668–676.